Characterization of 2.5 micron HgCdTe VIRGO/VISTA Detector Array

Craig W. McMurtry, Thomas S. Allen, Andrew C. Moore, William J. Forrest, and Judith L. Pipher

University of Rochester, Rochester, NY, USA

ABSTRACT

With the introduction of the Raytheon 2.5 micron HgCdTe VIRGO detector array, some astronomy programs, such as the VISTA Program, are turning to Raytheon for near infrared detector arrays. We characterize one VIRGO detector array and provide results of measurements at low backgrounds including dark current, read noise, total noise, quantum efficiency, and operability. The Raytheon VIRGO HgCdTe detector arrays are excellent candidates for many low background astronomical programs, including space-borne telescope missions.

Keywords: NIR, near infrared, detector array, HgCdTe, SNAP, VISTA, VIRGO, low noise, low dark current, ROIC, multiplexer, low background

1. INTRODUCTION

Recently, the VISTA Program (ground based application) reported[1] on the characterization of Raytheon $2.5\mu m$ HgCdTe VIRGO detector arrays, albeit at moderately high backgrounds. CalTech has similarly characterized the $2.5\mu m$ HgCdTe[2] and $1.7\mu m$ HgCdTe[3] detector arrays at low background levels for consideration in the SNAP Program which will employ $1.7\mu m$ HgCdTe detector arrays in a space-borne, low background application. We report on the results of low background measurements for a Raytheon HgCdTe infrared detector array with a cutoff wavelength of $2.5\mu m$. The $20\mu m$ pixel pitch HgCdTe detector array is bonded to the 2048×2048 pixel SB-301 ROIC (Read-Out Integrated Circuit or multiplexer). The detector array or SCA (Sensor Chip Assembly) tested is part number SB-301-027. Raytheon HgCdTe detector arrays have been shown to be mechanically stable over thousands of thermal cycles (Raytheon data). Further, the Raytheon ROICs do not exhibit burst noise or random telegraph noise.[4]

2. DATA

All data were taken with a pixel enable time of $10.0\mu s$ and pixel-to-pixel time of $10.4\mu s$ (includes pixel de-select and next pixel select) for a total frame time of $11.0s$ for the full 2048×2048 detector array using 4 outputs. Our array controller electronics have a noise floor of $10\mu V$ for Fowler-1 sampling[5] (or Correlated Double Sampling) and $\sim 3\mu V$ for Fowler-8 sampling.[6]

2.1. HgCdTe Detector Array Calibration

In order to obtain meaningful results, we needed to calibrate the HgCdTe SCAs. This involved the measurement of source follower gain, capacitance, linearity and well depth (or capacity). Unless otherwise stated, all measurements were obtained at 77.4K and an applied detector reverse bias of 500mV. The source follower gain of the SB-301 multiplexer is the product of gains from two series source follower FETs. The input reset voltage (Vrstuc) is varied while measuring output voltage (Vout), see Figure 1. The SB-301 ROIC has over 1 Volt of linear dynamic range.

We measured the pixel nodal capacitance using the variance versus signal method[7] with both small flux and total fluence levels ($< 5\%$ of well depth). The capacitance per pixel of this SCA is 40.3fF. The linearity of the detector is plotted in Figure 2, which is obtained using a small flux and integrating over successively longer times until saturation is reached. The well depth or capacity is given by the saturating fluence level obtained at

For further information, E-mail: craig.mcmurtry@rochester.edu

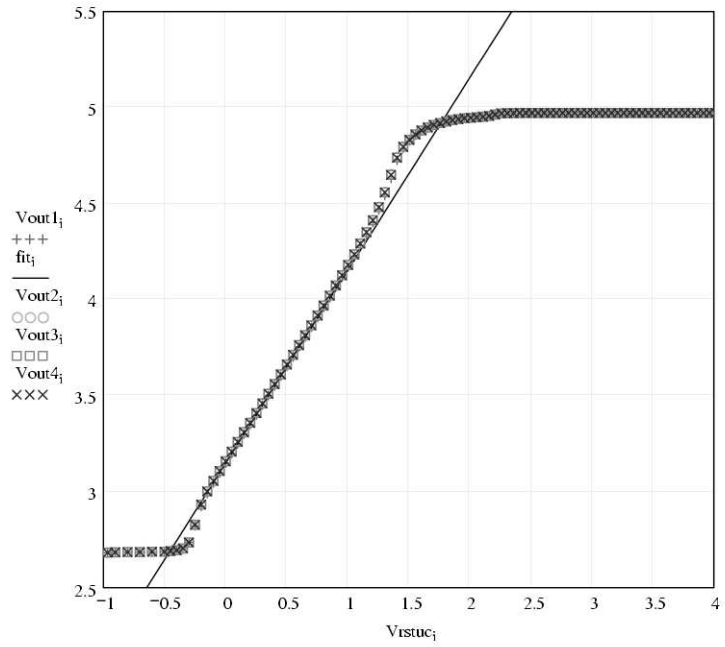

Figure 1. Source follower gain curve at 77.4K. The gain is 1.0 over the linear range. The departure from linear above Vrstuc voltage of 1.1V is due to the internal circuitry of the SB-301, specifically the clamp circuit, which is operating outside the normal range for this setting of Vrstuc.

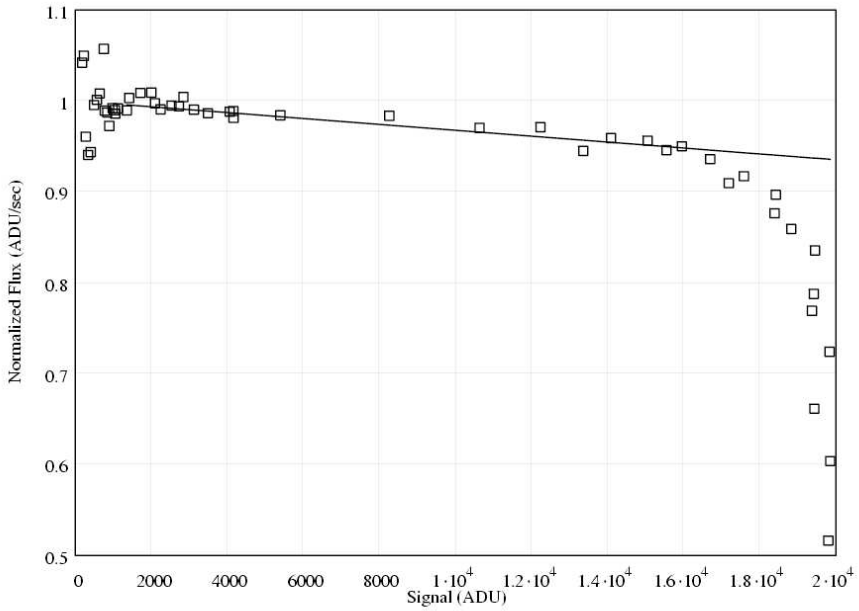

Figure 2. Linearity curve at 77.4K. We have plotted the normalized signal rate versus signal. The signal rate is given by the measured signal divided by the integration time. The signal rate is also commonly referred to as C_0/C, where the capacitance, C, varies with signal and is normalized using the capacitance at zero signal, C_0.

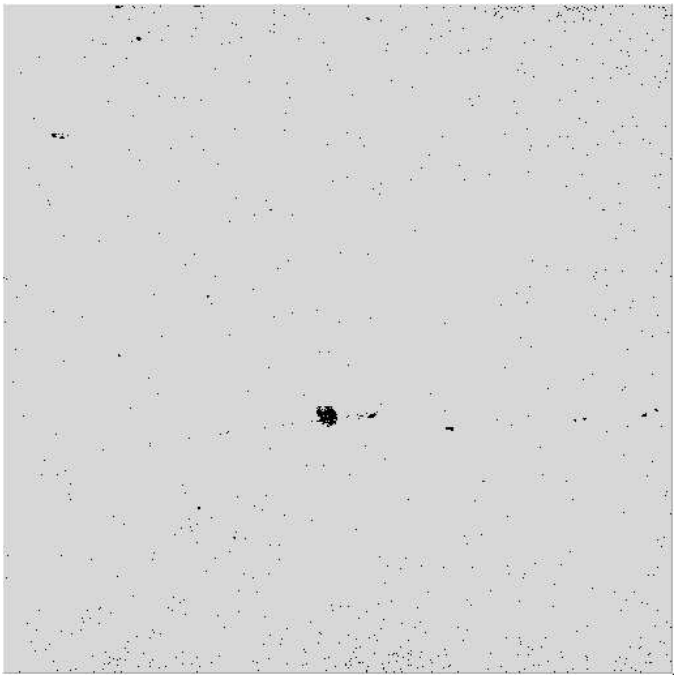

Figure 3. Image mask of operability for SCA 027. The vast majority of pixels are operable (gray), while only 0.45% (19039/4194304) are deemed inoperable (black).

the largest integration times used in the above linearity measurement and is 403mV or $105Ke^-$ at an applied detector reverse bias of 500mV. Due to the inherent non-linear nature of photo-voltaic detectors, large errors can arise in both conversion gain (capacitance) and quantum efficiency, as well as all measurements that apply the conversion gain (noise, dark current, etc.).[8] However, we have measured the capacitance at small signal levels and corrected all larger signal levels for such non-linearities, by applying the C_0/C correction given by the line fit in Figure 2. Following the methods given by Moore,[9] we measured the inter-pixel capacitance to be negligible for this Raytheon $2.5\mu m$ HgCdTe VIRGO detector array. The corrections implied by the measured inter-pixel capacitance to our conversion gain ($e^-/\mu V$) and total nodal capacitance are within the uncertainties of the measurements ($\sim 3\%$). Therefore, we have not applied interpixel capacitance corrections to our noise, dark current or quantum efficiency results. Our measured inter-pixel capacitance is consistent with the intra-pixel spot scan response reported by Smith[3] for a Raytheon HgCdTe VIRGO detector array.

The radiometric instability for this SCA was measured to be 0.28% over 1000 seconds. Using two basic criterion, we created an operability mask (see Figure 3). For a pixel to be labeled as inoperable, the pixel had to be dead (no response to light) and have dark current greater than $10e^-/sec$. The large dark current limit was chosen to eliminate confusion with cosmic ray hits during our more sensitive dark current measurements, while still allowing characterization of pixels with moderate and low dark currents. Under these constraints, the operability is 99.55%.

2.2. Dark Current

In the University of Rochester dewar, we have previously measured the light leak to be $< 0.002e^-/s$ over the $0.6\mu m$ to $5.4\mu m$ region. In order to accurately measure the dark current, we obtained dark charge versus integration time for integration times between 100 and 3000 seconds at T=77.4K. The use of reference pixels to subtract frame-to-frame drift due to slight temperature or bias fluctuations is vital to provide an accurate measurement of the dark current. The resultant dark current was measured on a pixel-by-pixel basis (see Figure 4). The median dark current is $0.029e^-/sec$. We did not attempt to isolate amplifier or multiplexer glow

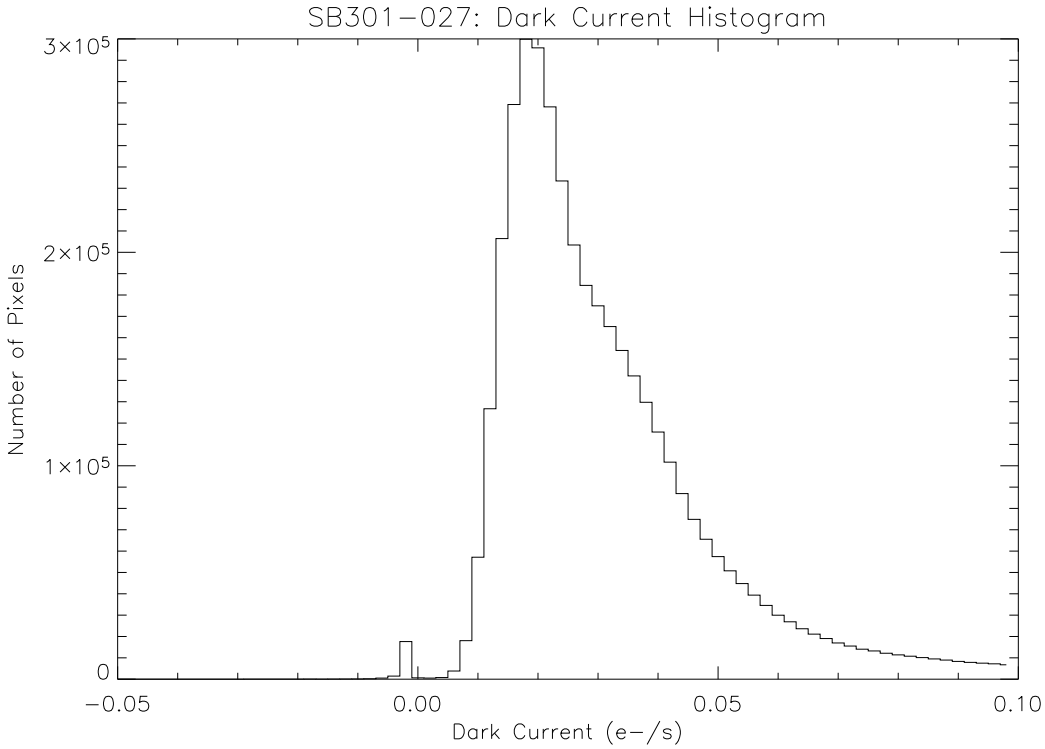

Figure 4. Histogram of dark current per pixel at 77.4K. The dark current distribution is nearly Gaussian with the exception of the higher dark current tail. This tail is typical of HgCdTe detector arrays, while InSb detector arrays exhibit dark current distributions that are much closer to Gaussian in shape.[6] The higher dark current pixels are distributed randomly across the array. The median dark current is $0.029e^-/sec$. The applied detector reverse bias was $500mV$, which corresponds to an actual well depth of $403mV$ or $105Ke^-$.

from the dark current measurements, since the dark current per pixel distribution across the array is nearly uniform.

To determine if Raytheon's HgCdTe detector array processing is producing the lowest dark current detector arrays possible, we needed to understand the mechanisms responsible for the dark current. To this end, we measured the dark current versus temperature for the $2.5\mu m$ SCA 027 (see Figure 5). The data between T=125K and 90K in Figure 5 clearly show that SCA 027 is limited by generation-recombination dark current and not surface currents. Near liquid nitrogen temperatures, the dark current versus temperature has flattened out. Since our measured light leak levels are significantly less than the measured dark current, we believe that the dark current near T=77K is indicative of trap-assisted tunneling. However, more data at lower temperatures and at different applied detector reverse biases are needed to fully constrain the theoretical models. Nevertheless, the measured dark current at the three lowest temperatures is well fit by the sum of the dark current models. Therefore, Raytheon's HgCdTe detector array processing would need to reduce impurities (i.e. reduce trap densities) to produce even lower dark current detector arrays. Alternatively, a lower applied reverse detector bias (and consequently lower well depth) could be employed to reduce the dark current, since the trap-assisted tunneling dark current is very bias dependent.

For the SNAP Program, the near infrared detector arrays under consideration are $1.7\mu m$ HgCdTe detector arrays operating at T=140K. The required dark current for this mission is $< 0.2e^-/s$. Recently Raytheon has measured $0.25e^-/s$ dark current for a $1.8\mu m$ HgCdTe detector array operating at T=140K. Based upon our dark current models, Raytheon is capable of producing a $1.7\mu m$ detector array that meets the $< 0.2e^-/s$ dark current requirement (see Figure 6).

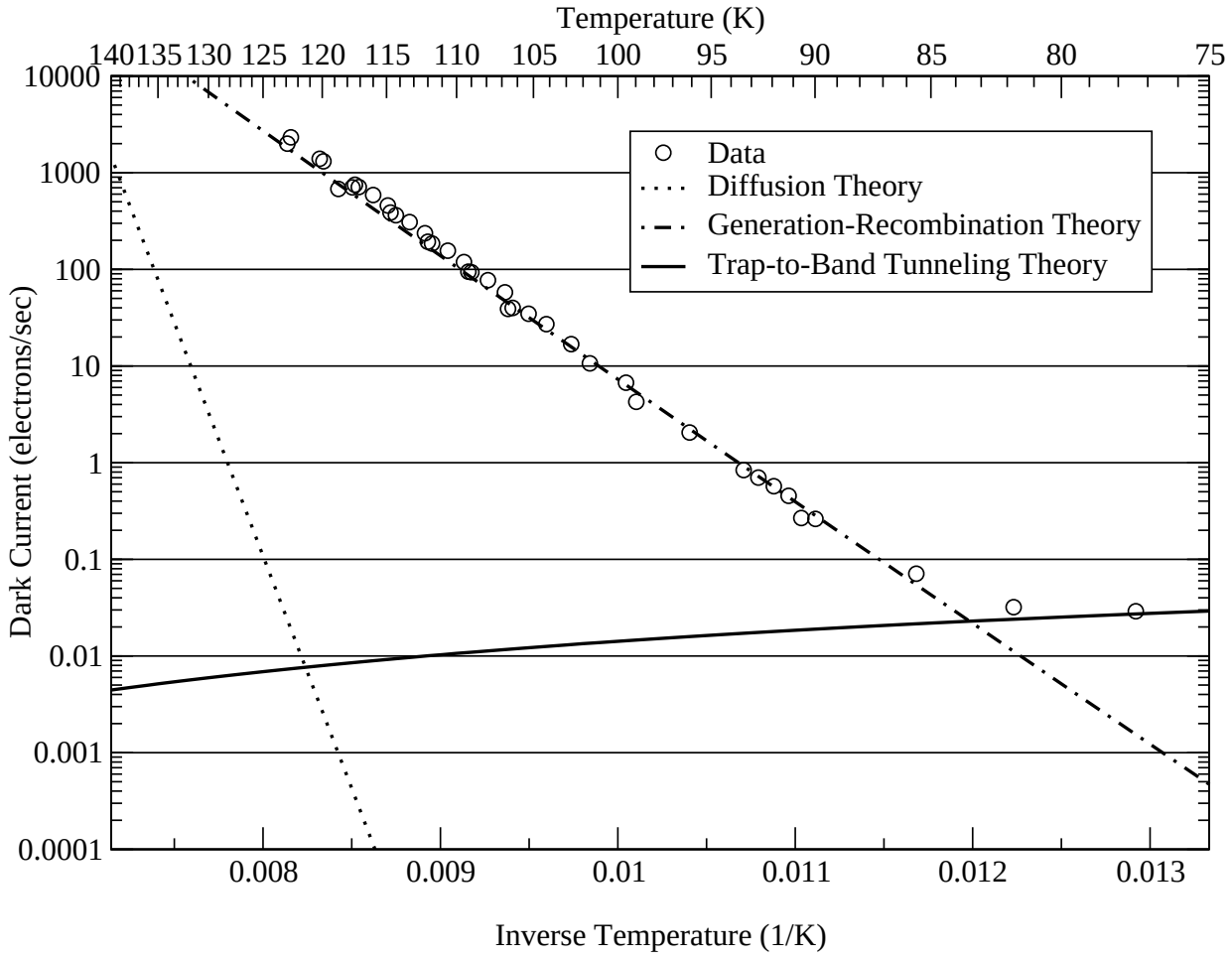

Figure 5. Measured dark current per pixel versus temperature, with theoretical plots for diffusion, generation-recombination and trap assisted tunneling dark currents for $2.5\mu m$ HgCdTe SCA 027. The applied detector reverse bias was $500mV$, which corresponds to an actual well depth of $403mV$ or $105Ke^-$.

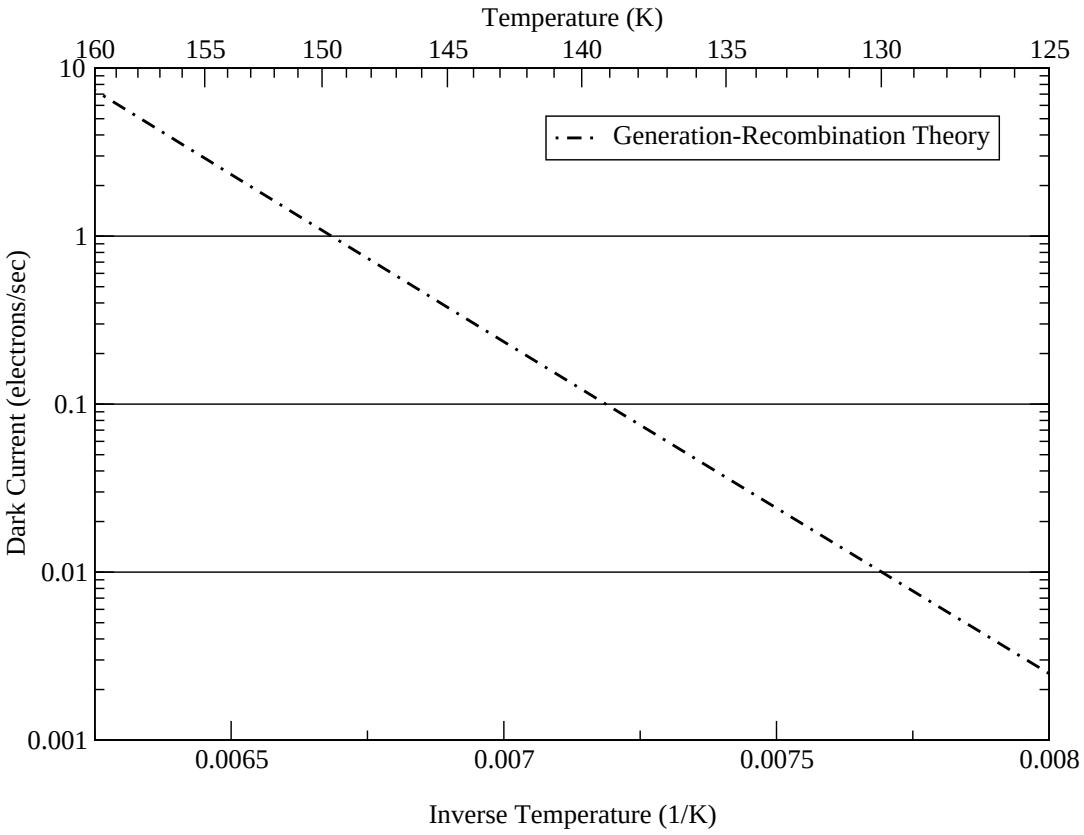

Figure 6. Theoretical Generation-Recombination dark current per pixel versus temperature for a $1.7\mu m$ wavelength cutoff HgCdTe detector array. No data were measured using $1.7\mu m$ HgCdTe detector arrays, instead the theory is based upon our models for the $2.5\mu m$ HgCdTe detector arrays, with changes to the appropriate parameters. This graph is illustrative only, i.e. what dark current could be expected for an array that operates at T=140K for the SNAP Program.

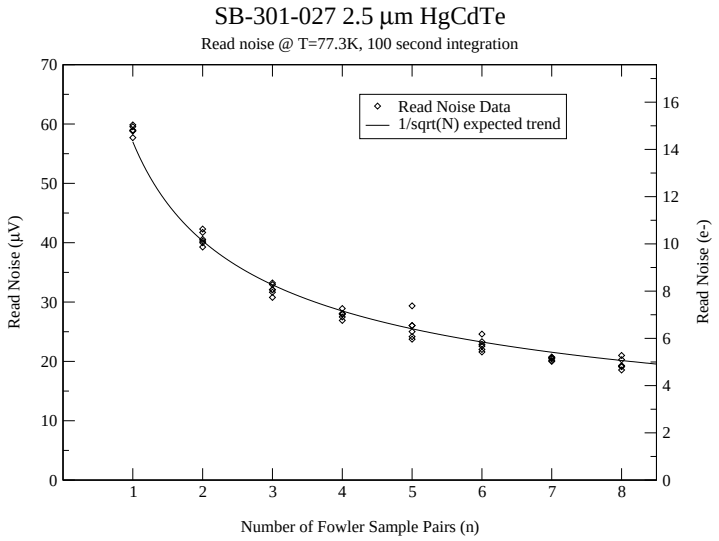

Figure 7. Read noise versus Fowler Sampling. All data are taken at 77.4K with 100 seconds integration time so that dark current does not contribute to the noise. The data follow the expected $1/\sqrt{N}$ curve for increasing N samples.

2.3. Noise

The read noise was measured in regimes where the dark current makes little or no contribution to the total noise, i.e. at sufficiently short integration times. We have measured the read noise using the "zero mean" method, i.e. the {standard deviation / $\sqrt{2}$ } in a sub-array from the difference of two images, where the expected mean is zero (see Figure 7). For a single Fowler pair read, or a correlated double sample (CDS) read, SCA 027 had an average read noise of $14.8e^-$. At Fowler-8 sampling, the average read noise was reduced to $4.9e^-$.

While the read noise and dark current often give a good estimate to the total noise expected for a given observation, the true total noise is typically larger than the quadrature sum of the read noise and the shot noise in the dark charge. The source of the excess noise is usually 1/f noise.[10] Therefore, we have measured the total noise in a 1000sec Fowler-8 sampled dark image and found the average total noise to be $8.7e^-$.

To continue the comparison of $1.7\mu m$ HgCdTe detector arrays operating at T=140K, we have measured the read noise of ROICs (bare multiplexers). At T=140K, the ROIC would have a slightly lower read noise than that given above for the T=77.4K operation. After scaling the noise voltage of the bare ROIC to that of a full detector array, we find the CDS read noise is $14.6e^-$ and using Fowler-8 sampling, the read noise is $4.8e^-$.

2.4. Quantum Efficiency

To accurately measure the quantum efficiency (QE), we used a dewar with the simplest possible optical path and therefore the simplest possible $A\Omega$. The optical path from the outside of the dewar to the detector consists of 1) the dewar window, 2) liquid nitrogen shield, 3) liquid helium shield, 4) filter, and 5) circular aperture stop. The two cryogenic shields have circular openings that are sufficiently large such that they are well outside of the optical path. For flood illumination, $A\Omega$ is therefore determined by the pixel area, aperture stop area and distance between the pixel and the aperture. The QE data were corrected for $\cos^4\theta$ effects. The responsive quantum efficiency (RQE) is given by:

$$RQE = \frac{S}{S_0}, \tag{1}$$

Table 1. Responsive Quantum Efficiency and Detective Quantum Efficiency measured using astronomical broad band filters J, H, and K. While DQE > RQE is unphysical, the difference between the two measurements represents the uncertainty in the measurements.

λ_c	$1.255\mu m$	$1.645\mu m$	$2.19\mu m$
$\Delta\lambda$	$0.298\mu m$	$0.332\mu m$	$0.41\mu m$
RQE	87%	86%	87%
DQE	90%	90%	90%

and detective quantum efficiency (DQE) by:

$$DQE = \frac{(\frac{S}{N})^2}{S_0}, \tag{2}$$

where S is the measured signal (in photons) from the detector, S_0 is the actual signal (in photons, given by black body source, filter transmission and $A\Omega$), and N is the noise obtained via the standard deviation of the difference of two signal measurements. The RQE results can be larger than 100% if photo-conductive gain is present, while DQE $\leq$ 100%. In addition, the DQE measurements are not subject to errors in the capacitance measurements.

The cold IR filters in the University of Rochester dewar are all from OCLI or Barr and have transmission traces both at room temperature and at 77K. For $1.0\mu m < \lambda < 3.0\mu m$, the QE was measured using a NIST calibrated black body (Omega BB-4A, 100 - 1000°C, $\varepsilon = 0.99$), see Table 1. Raytheon has produced an excellent anti-reflective coating for their HgCdTe detector arrays which demonstrates both a high absolute QE and a flat response over the $1 - 2.5\mu m$ region, i.e. no "roll-off" at shorter wavelengths.

3. CONCLUSIONS

The Raytheon SCA 027 has $0.029e^-/s$ dark current at T=77.4K with a large well depth ($> 100Ke^-$). Furthermore, the read noise of this SCA is $14.8e^-$ (CDS) and $4.9e^-$ (Fowler-8). The quantum efficiency is 90% over the entire near infrared region. We have shown that the Raytheon $2.5\mu m$ HgCdTe detector arrays are excellent low noise, low dark current and high quantum efficiency detector arrays which are well suited for many low background applications, including space borne astronomical telescope missions.

In comparison, the Raytheon $1.7\mu m$ HgCdTe detector arrays, operating at T=140K, would provide a read noise of $14.6e^-$ (CDS) and $4.8e^-$ (Fowler-8 sampling). Based upon our measurements of dark current for longer wavelength arrays, the dark current for a $1.7\mu m$ HgCdTe array operating at T=140K would be $< 0.2e^-/s$. The quantum efficiency versus wavelength is both high (90%) and flat over the near infrared region. The Raytheon $1.7\mu m$ HgCdTe VIRGO detector arrays would perform well if selected as the detector arrays for the SNAP program.

REFERENCES

1. N. Bezawada, D. Ives, and G. Woodhouse, "Characterisation of VISTA IR detectors," in *Proc. SPIE, Optical and Infrared Detectors for Astronomy*, J. D. Garnett and J. W. Beletic, eds., **5499**, pp. 23–34, 2004.
2. R. Smith, M. Bonati, and D. Guzman, "VIRGO-2K $2.5\mu m$ HgCdTe Dark Current," in *Proc. SPIE, Optical and Infrared Detectors for Astronomy*, J. D. Garnett and J. W. Beletic, eds., **5499**, pp. 119–130, 2004.
3. R. Smith, "Characterization of $1.7\mu m$ cutoff detectors for SNAP," in *Workshop on Scientific Detectors for Astronomy, Springer-Verlag*, **in press**, 2005.
4. C. M. Bacon, C. W. McMurtry, J. L. Pipher, W. J. Forrest, and J. D. Garnett, "Burst noise in the HAWAII-1RG multiplexer," in *Proc. SPIE, Focal Plane Arrays for Space Telescopes II*, T. J. Grycewicz and C. J. Marshall, eds., **5902**, pp. in press, these proceedings, 2005.

5. A. M. Fowler and I. Gatley, "Noise reduction strategy for hybrid IR focal-plane arrays," in *Proc. SPIE, Infrared Sensors: Detectors, Electronics, and Signal Processing*, T. S. Jayadev, ed., **1541**, pp. 127–133, 1991.
6. C. W. McMurtry, W. J. Forrest, A. C. Moore, and J. L. Pipher, "James Webb Space Telescope: Characterization of Flight Candidate NIR InSb Detector Arrays," in *Proc. SPIE, Focal Plane Arrays for Space Telescopes*, T. J. Grycewicz and C. R. McCreight, eds., **5167**, pp. 144–158, 2003.
7. L. Mortara and A. Fowler, "Evaluations of CCD: Performance for Astronomical Use," *Proc. SPIE, Solid State Imagers for Astronomy* **290**, pp. 28–30, 1981.
8. B. Pain and B. Hancock, "Accurate Estimation of Conversion Gain and Quantum Efficiency in CMOS Imagers," in *Proc. SPIE, Sensors and Camera Systems for Scientific, Industrial, and Digital Photography Applications IV*, M. Blouke, N. Sampat, and R. Motta, eds., **5017**, pp. 94–103, 2003.
9. A. C. Moore, Z. Ninkov, and W. J. Forrest, "Interpixel Capacitance in Nondestructive Read-out Focal Plane Arrays," in *Proc. SPIE, Focal Plane Arrays for Space Telescopes*, T. J. Grycewicz and C. R. McCreight, eds., **5167**, pp. 204–215, 2003.
10. C. W. McMurtry, W. J. Forrest, and J. L. Pipher, "James Webb Space Telescope: Noise Results for the Multiplexers of the Mid-Infrared Instrument (MIRI)," in *Proc. SPIE, Focal Plane Arrays for Space Telescopes II*, T. J. Grycewicz and C. J. Marshall, eds., **5902**, pp. in press, these proceedings, 2005.